

named as H, I, J and L, respectively. The center of halo, \vec{R}_G , is defined by the following way to be presented by a mark of + . $\vec{R}_G = \sum \vec{r}_i D_i / \sum D_i$, where D_i and \vec{r}_i , respectively, represent the darkness and position vector of each cell.

2-2) Determination of incident direction

As an air family generally comes into the chamber with inclined direction and halo looks like an elliptical shape which extends to the incident direction, the correction for inclined incidence must be made. For the correction, we make the following way. One subtracts the $D = D_0(x_0, y_0) \exp(-r/r_0)$, (x_0, y_0) is the position of halo center and r_0 is arbitrary, from the all D_i of the cell. As the function, $D = D_0 \exp(-r/r_0)$, is a circular symmetrical one on r , subtraction of this function from elliptical halo makes the plus area in both edge of long axis of ellipse and the minus area in both edge of short axis of ellipse when we chose suitable size of r_0 . If we can get a line which is joined at two plus area, we determine the direction of the line as incident one and correction for inclined direction is made along the direction. In fact, the coefficient of correlation, R_{xy} , of the first degree is calculated and in the case when absolute value of it is greater than 0.5, we consider there is a linear correlation on x and y and determine the line of incident direction by the least square method.

2-3) Subtraction of the core from halo

We assume that the lateral distribution of the darkness of the core is $D(r, x, y, r_0) dr = D_0(x, y) \exp(-r/r_0) 2\pi r dr$, and we input the position of the core, (x, y) , and its mean spread, r_0 . D_0 is the darkness of the core center and we can get the electron density, ρ_0 ($1/\text{cm}^2$) at $r=0$ by transforming D_0 to ρ_0 .

The distribution, $D(r, x, y, r_0)$, thus defined is subtracted from the darkness of halo made of 80×80 cells (contour map) at each r in order of the magnitude of the core size and new contour map is constructed. In this time, correction for inclined incidence is made with the way described in preceding paragraph. Fig.2 shows the new map thus obtained by subtraction of the highest energy core L on the assumption of $r_0 = 1.5$ mm. In the figure, we can see the core L disappears and H, I and J cores survive. The same procedures are applied to the second highest core J with $r_0 = 1.5$ mm and to the cores H, I with $r_0 = 0.5$ mm, respectively and the new map are shown in Fig.3. In the figure we can see all the four cores disappear.

3 Discussion

Table 1 shows the summary of some quantity on cores H, I, J and L thus obtained. In the Table 1, ρ_0 and R_0 present electron density of the cores at $r=0$ and mean lateral spread of the cores, respectively. R is the distance from the center of halo to the core and N_e is a total electron number in the core obtained by $N_e = \int_0^\infty \rho_0 e^{-r/r_0} 2\pi r dr$. According to the simulation calculation by Makio Shibata, we can get the energy of core by transforming the number of electrons in core at 10 c.u. to the energy(8). E in Table 1 shows the energy of each core thus estimated. R_{ij} is a relative distance among each core and Z_{ij} is a quantity induced by Pamir group as $Z_{ij} = R_{ij} (1/N_i + 1/N_j)^{-1}$, which is connected with the relative transverse momentum of each core(6)(7). ER_{ij} is the relative lateral spread of each core obtained by $R_{ij} (1/E_i + 1/E_j)^{-1}$ using the energy of the cores instead of N_i . Fig.4 shows the scatter plot of

the cores in E-R diagram together with that of computer-constructed A-jets. The triangles with capital letters H, I, J and L show the plots of the cores of M.A.III and the closed circles with small letter i, j and l show the A-jets of M.A.III which should correspond to the cores I, J and L as seen in ref.(5). The cores J and L well correspond to the A-jets j and l but correspondence of the core I to A-jet i is not so good. We suppose it is caused by using the unfit r_0 . The core H is originated from hadronic component as seen in ref.(5) and the shower development does not still reach the maximum at 10 c.u..

This report is preliminary one and shows the new method of investigation of the core structure. There remain problems to be solved, such as the way of determination of r_0 , the order of subtraction of the cores and derivation of the P_t from Z_{1j} , etc.. These problems are under considerations and we will make the answer on their problems in separate publication.

Acknowledgment

The authors would like to express their thanks to all the members of Chacaltaya emulsion chamber experiment. Special thanks are also to Profs. Y. Fujimoto and S. Hasegawa for their kind advices.

Figure captions

- Fig.1: Contour map of halo in RR-type X-ray film at 10 c.u. on M.A.III. Cores H, I, J and L are recognized in it. Darkness are shown by numerals in figure.
- Fig.2: Contour map of halo on M.A.III after subtracting the core L from Fig.1 with $R_0=1.5$ mm.
- Fig.3: Contour map of halo on M.A.III after subtracting the core J from Fig.2 with $R_0=1.5$ mm and the cores H and I with $R_0=0.5$ mm.
- Fig.4: Scatter plot of the cores in E-R diagram together with that of computer-constructed A-jet. Marks are \triangle for the cores of M.A.III, \circ for A jet of Andromeda, \times for A-jet of Ursa Maior and \bullet for A-jet of M.A.III.

Reference

- (1) A. Ohsawa: ICR-Report-112-83-6(1983)65
- (2) J.A.Chinellato: Dr Thesis; Universidade Estadual de Campinas (1981).
- (3) K. Sawayanagi : Proc. Int. Sym. on Cosmic Ray and Particle Physics , Tokyo (1984)116.
- (4) N.M. Amato et al.: Proc. Int. Sym. on Cosmic Rays and Particle Physics (1984)123.
- (5) S. Yamashita: Jour. of the Phys. Soci. of Japan Vol.54 No.2(1985) 529.
- (6) Pamir collaboration: Proc. 18th Int. Cosmic-Ray Conf. Vol.5 (1983)126.
- (7) L.T. Baradzei et al.: Proc Int. Sym. on Cosmic Rays and Particle Physics, Tokyo(1984)136.
- (8) M. Shibata et al.:Uchusen Kenkyu(in Japanese) Vol.26 No.4(1983)13

Table 1

#	$\rho_0 (1/\text{cm}^2)$	$R_0 (\text{mm})$	$R (\text{mm})$	N_e	$E (\text{TeV})$
L	2.63×10^7	1.5	1.65	3.72×10^6	580
J	1.91×10^7	1.5	0.55	2.69×10^6	420
H	2.27×10^7	0.5	2.84	3.56×10^5	56
I	6.25×10^6	0.5	1.86	9.81×10^4	15

#--#	$R_{ij} (\text{mm})$	$Z_{ij} (\text{els.mm})$	$ER_{ij} (\text{TeV.mm})$
L--J	2.20	3.44×10^6	536
L--H	3.67	1.19×10^6	187
L--I	3.13	2.99×10^5	46
J--H	2.66	8.37×10^5	131
J--I	1.54	1.46×10^5	22
H--I	1.24	9.58×10^4	14

Fig.1

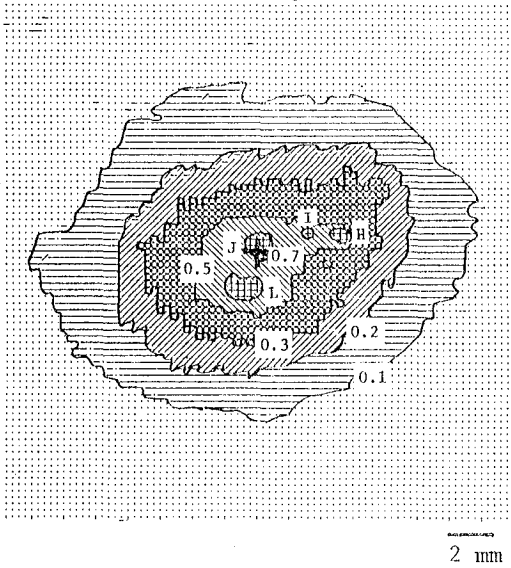


Fig.2

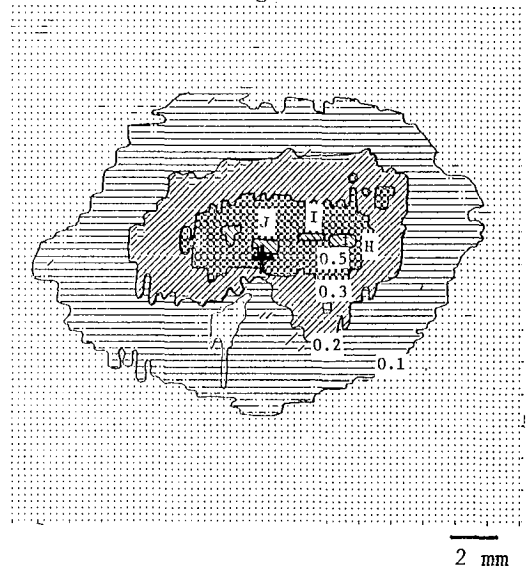


Fig.3

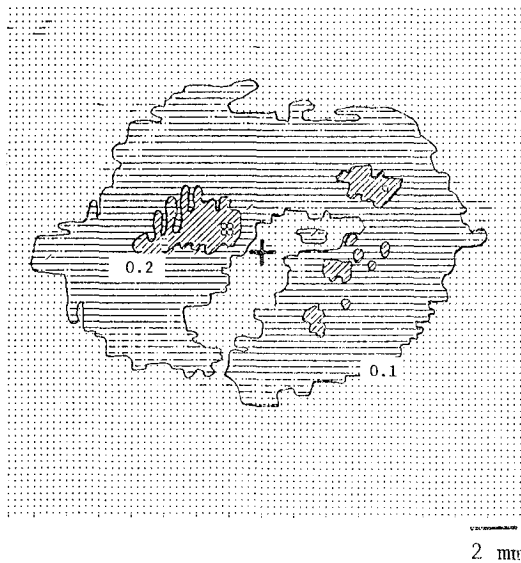


Fig.4

